



Published in final edited form as:

ACS Chem Biol. 2018 August 17; 13(8): 2300–2307. doi:10.1021/acscchembio.8b00463.

## Cytochrome *c* Reduction by H<sub>2</sub>S Potentiates Sulfide Signaling

Victor Vitvitsky<sup>†</sup>, Jan Lj. Miljkovic<sup>‡,§,#</sup>, Trevor Bostelaar<sup>†</sup>, Bikash Adhikari<sup>‡,§</sup>, Pramod K. Yadav<sup>†</sup>, Andrea K. Steiger<sup>||</sup>, Roberta Torregrossa<sup>⊥</sup>, Michael D. Pluth<sup>||</sup>, Matthew Whiteman<sup>⊥</sup>, Ruma Banerjee<sup>\*†</sup>, and Milos R. Filipovic<sup>\*,‡,§</sup>

<sup>†</sup>Department of Biological Chemistry, University of Michigan, Ann Arbor, Michigan 48109, United States

<sup>‡</sup>Université de Bordeaux, IBGC, UMR 5095, F-33077 Bordeaux, France

<sup>§</sup>CNRS, IBGC, UMR 5095, F-33077 Bordeaux, France

<sup>||</sup>Department of Chemistry and Biochemistry, Institute of Molecular Biology, and Materials Science Institute, University of Oregon, Eugene, Oregon 97403, United States

<sup>⊥</sup>University of Exeter Medical School, St. Luke's Campus, Exeter EX1 2LU, U.K.

### Abstract

Hydrogen sulfide (H<sub>2</sub>S) is an endogenously produced gas that is toxic at high concentrations. It is eliminated by a dedicated mitochondrial sulfide oxidation pathway, which connects to the electron transfer chain at the level of complex III. Direct reduction of cytochrome *c* (Cyt C) by H<sub>2</sub>S has been reported previously but not characterized. In this study, we demonstrate that reduction of ferric Cyt C by H<sub>2</sub>S exhibits hysteretic behavior, which suggests the involvement of reactive sulfur species in the reduction process and is consistent with a reaction stoichiometry of 1.5 mol of Cyt C reduced/mol of H<sub>2</sub>S oxidized. H<sub>2</sub>S increases O<sub>2</sub> consumption by human cells (HT29 and HepG2) treated with the complex III inhibitor antimycin A, which is consistent with the entry of sulfide-derived electrons at the level of complex IV. Cyt C-dependent H<sub>2</sub>S oxidation stimulated protein persulfidation in vitro, while silencing of Cyt C expression decreased mitochondrial protein persulfidation in a cell culture. Cyt C released during apoptosis was correlated with persulfidation

\*Corresponding Authors milos.filipovic@ibgc.cnrs.fr., rbanerje@umich.edu.

#Present Address: J.Lj.M.: Department of Genetics and Complex Diseases, Harvard TH Chan School of Public Health, Boston, MA.

#### Author Contributions

V.V. designed experiments, performed spectral analysis of the interaction of Cyt C with sulfide and hydrodisulfide, determined the pH dependence of Cyt C reaction with sulfide, performed the oxygen consumption assays, performed data analysis, and wrote the manuscript. J.Lj.M. performed experiments with Cyt C siRNA, fluorescence microscopy, caspase activity, flow cytometry, and mitochondrial persulfidation, performed data analysis, and wrote the manuscript. T.B. performed oxygen consumption assays with Cyt C, performed data analysis, and wrote the manuscript. B.A. performed fluorescence microscopy, H<sub>2</sub>S measurements, and HSA persulfidation. P.K.Y. performed and analyzed the stopped-flow kinetic studies. A.K.S., M.D.P., R.T., and M.W. contributed new analytical tools. M.D.P. and M.W. co-wrote the manuscript. R.B. helped design kinetic, spectroscopic, and OCR experiments, analyzed the data, and co-wrote the manuscript. M.R.F. designed experiments, performed mass spectrometry, performed persulfidation of ATR and ETHE1, performed data analysis, and wrote the manuscript.

The authors declare the following competing financial interest(s): M.W. has patents on the therapeutic and agricultural use of mitochondrially targeted, and other, hydrogen sulfide delivery molecules.

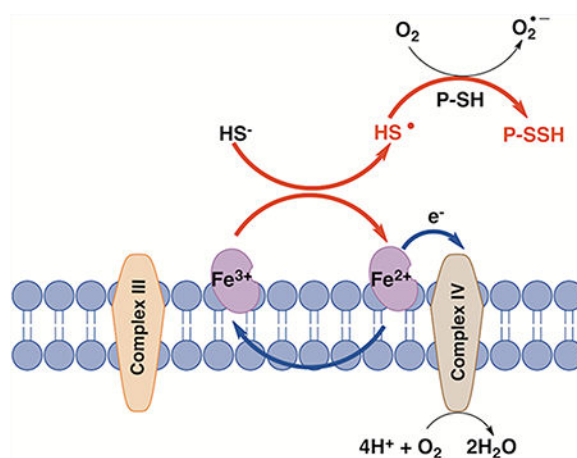
#### ASSOCIATED CONTENT

##### Supporting Information

The Supporting Information is available free of charge on the ACS Publications website at DOI: 10.1021/acscchembio.8b00463. Supporting Figures 1–5, Supporting Materials and Methods, and references (PDF)

of procaspase 9 and with loss of its activity. These results reveal a potential role for the electron transfer chain in general, and Cyt C in particular, for potentiating sulfide-based signaling.

### Graphical Abstract:



H<sub>2</sub>S is an energy source for prokaryotes adapted for life in sulfide rich environments, but it is a potent respiratory toxin for other organisms. The targets of H<sub>2</sub>S poisoning are the metal centers in cytochrome *c* oxidase, the terminal station in the mitochondrial electron transfer chain (ETC).<sup>1,2</sup> At low concentrations, however, H<sub>2</sub>S modulates physiological processes ranging from inflammation to cardiovascular function and apoptosis.<sup>3-5</sup> Cellular H<sub>2</sub>S levels must therefore be maintained within a nontoxic window by regulating enzymes involved in its biogenesis<sup>6-9</sup> and degradation.<sup>10,11</sup> The mitochondrial sulfide oxidation pathway transfers electrons from H<sub>2</sub>S oxidation to complex III via coenzyme Q.<sup>12</sup> In red blood cells lacking mitochondria, a noncanonical sulfide oxidation route uses ferric hemoglobin and catalyzes conversion of H<sub>2</sub>S to thiosulfate.<sup>13</sup> Polysulfides that are also produced in this reaction are degraded by reductants such as glutathione.<sup>14</sup> Other heme proteins like myoglobin<sup>15</sup> and neuroglobin<sup>16</sup> also catalyze ferric heme-dependent H<sub>2</sub>S oxidation. Unlike hemoglobin and myoglobin, H<sub>2</sub>S oxidation by neuroglobin, in which the heme has two axial histidine ligands, does not involve direct coordination of sulfide to ferric iron.

Cytochrome *c* (Cyt C) resides in the mitochondrial intermembrane space and shuttles electrons between complexes III and IV in the ETC. Release of Cyt C into the cytosol triggers apoptotic activation of caspase 9.<sup>17</sup> As in neuroglobin, the heme in Cyt C is six-coordinate and exhibits bis-His or His/Met ligation. In principle, electrons from the oxidation of H<sub>2</sub>S can enter the ETC at the level of complex IV either directly<sup>18</sup> or indirectly via initial reduction of ferric Cyt C by sulfide.<sup>19</sup> However, the standard redox potential for the S<sup>•-</sup>, H<sup>+</sup>/HS<sup>-</sup> couple is +0.91 V (vs NHE)<sup>20</sup> compared to +0.26 V for Cyt C,<sup>21</sup> rendering reduction of Cyt C by H<sub>2</sub>S thermodynamically unfavorable. However, reduction of Cyt C by sulfide has been observed *in vitro*<sup>19,22</sup> and in the ciliated gills of *Guenkensia demissa*, a mussel that lives in sulfide rich sediments.<sup>23</sup> An additional link between H<sub>2</sub>S and Cyt C was reported in a study on rotenone-induced apoptosis in which H<sub>2</sub>S exposure preserved mitochondrial function, limited Cyt C release, and inhibited dissipation of the mitochondrial

proton membrane potential.<sup>24</sup> However, a quantitative analysis of H<sub>2</sub>S oxidation by Cyt C, identification of the reaction products, and elucidation of its effects on apoptosis and persulfide signaling has been lacking.

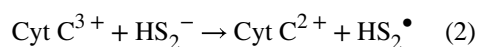
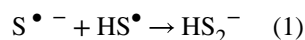
In this study, we report the kinetics of Cyt C reduction by H<sub>2</sub>S, demonstrate formation of thiosulfate as a reaction product, and show stimulation of O<sub>2</sub> consumption in human cells treated with antimycin A, consistent with the delivery of electrons from H<sub>2</sub>S to complex IV via Cyt C. We also demonstrate that Cyt C in the presence of H<sub>2</sub>S stimulates protein persulfidation, suggesting a potentiating role of the ETC in H<sub>2</sub>S-dependent signaling in general and in regulation of apoptosis via persulfidation of caspase 9 in particular.

## RESULTS AND DISCUSSION

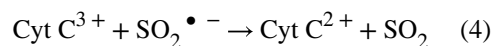
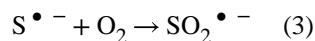
### Kinetics of Cyt C Reduction by Sulfide.

Addition of stoichiometric H<sub>2</sub>S to ferric Cyt C (Soret band at 409 nm) results in its complete conversion to the ferrous form (415 nm) with sharpening of the  $\alpha/\beta$  bands at 550 and 520 nm (Figure 1A). The kinetics of Cyt C reduction by sulfide exhibits a pronounced lag phase (Figure 1B), indicating that the reaction either involves a slow step (e.g., ligand exchange from histidine to HS<sup>-</sup>) or is accelerated as H<sub>2</sub>S oxidation products accumulate. Cryo-ESI MS previously used to observe HS<sup>-</sup> coordination to ferric heme<sup>15</sup> did not identify a comparable adduct with Cyt C (Supporting Figure 1). The stoichiometry of the reduction reaction (1.5:1.0 Cyt C:sulfide) was independent of the presence of O<sub>2</sub> (Figure 1C). The Cyt C reduction rate showed a bell-shaped dependence on pH with a maximum at 7.5 and inflection points at  $6.7 \pm 0.1$  and  $8.5 \pm 0.1$  (Figure 1D). Phosphate and citrate buffers, previously shown to bind Cyt C and influence its overall charge and redox potential,<sup>25</sup> significantly inhibited the rate of ferric Cyt C reduction by sulfide (not shown).

As discussed above, the one-electron reduction of Cyt C with HS<sup>-</sup> is thermodynamically unfavorable, which could explain the observed lag phase (Figure 1B). In principle, HS<sup>•</sup>/S<sup>•-</sup> could dimerize at a diffusion-controlled rate ( $k = 9 \times 10^9 \text{ M}^{-1} \text{ s}^{-1}$ )<sup>2</sup> giving HS<sub>2</sub><sup>-</sup> (eq 1). However, the probability of HS<sup>•</sup>/S<sup>•-</sup> reaching sufficiently high concentrations for the dimerization reaction is likely to be low. Furthermore, formation of HS<sub>2</sub><sup>-</sup> would not provide the driving force for Cyt C reduction, as the reaction (eq 2) is thermoneutral [ $E^{\circ'}$ (Cyt C<sup>3+</sup>/Cyt C<sup>2+</sup>) = +0.26 V, and  $E^{\circ'}$ (S<sub>2</sub><sup>•-</sup>, H<sup>+</sup>/HS<sub>2</sub><sup>-</sup>) = +0.27 V].<sup>2,20</sup>



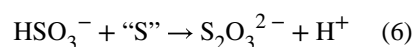
Alternatively, O<sub>2</sub> could react with the initially formed HS<sup>•</sup>/S<sup>•-</sup> at a diffusion-controlled rate ( $k = 5 \times 10^9 \text{ M}^{-1} \text{ s}^{-1}$ )<sup>2</sup> to produce SO<sub>2</sub><sup>•-</sup>, a strong reducing agent (eqs 3 and 4). However, the extent of Cyt C reduction was independent of O<sub>2</sub> (Figure 1C).



An alternative mechanism for explaining the hysteretic behavior is that the initially formed  $\text{HS}^{\bullet}/\text{S}^{\bullet -}$  reacts with  $\text{HS}^-$  ( $k_{\text{on}} = 4 \times 10^9 \text{ M}^{-1} \text{ s}^{-1}$ , and  $k_{\text{off}} = 5 \times 10^3 \text{ M}^{-1} \text{ s}^{-1}$ )<sup>2,20</sup> forming  $\text{H}_2\text{S}_2^{\bullet -}$ , which is a strong reducing agent [ $E^{\circ'}(\text{HS}_2^{\bullet -}, \text{H}^+/\text{H}_2\text{S}_2^{\bullet -}) = -1.13 \text{ V}$ ]<sup>2,20</sup> and could pull the Cyt C reduction reaction forward. Interestingly,  $\text{Na}_2\text{S}_2$  reduced Cyt C more rapidly than sulfide and do so without an observable lag phase (Figure 2A).

### Degradation of Excess Sulfide in the Presence of Cyt C.

Biphasic  $\text{O}_2$  consumption kinetics were seen when Cyt C was mixed with excess sulfide (Figure 2B). As the ratio of sulfide to Cyt C concentration was increased, the amplitude of the initial burst phase and the slope of the slow phase increased. These data are consistent with the model in which the burst phase corresponds to the reduction of Cyt C during which the initially formed  $\text{HS}^{\bullet}/\text{S}^{\bullet -}$  is rapidly oxidized, while the slow phase represents subsequent oxidation reactions. The amplitude of the burst phase showed a hyperbolic dependence on sulfide concentration and asymptotically approached 0.7 equiv of Cyt C to  $\text{O}_2$  consumed (Figure 2C). Biphasic  $\text{O}_2$  consumption suggested formation of products with higher sulfur oxidation states.  $\text{SO}_2$  formation (eq 4) would result in accumulation of sulfite, which in the presence of a sulfane sulfur donor (“S”) would form thiosulfate as a final product (eqs 5 and 6).<sup>2</sup>

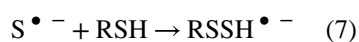


We tested for the formation of sulfide oxidation products under aerobic conditions (Figure 2D). Loss of sulfide was paralleled by the accumulation of thiosulfate and, to a lesser degree, sulfite. The recovery of sulfur equivalents in the thiosulfate, which has two sulfur atoms ( $\sim 280 \mu\text{M}$ ), and sulfite ( $\sim 40 \mu\text{M}$ ) pools represent  $\sim 50\%$  of the sulfide lost. Because of the interference of Cyt C with the cold cyanolysis method, we were unable to evaluate the concentration of sulfane sulfur species in the reaction mixture. ESI-TOF MS in the negative mode confirmed formation of thiosulfate and also revealed the presence of sulfate (Figure 2E). Although sulfite was not seen (possibly because of its low  $m/z$ ), we detected the sulfur trioxide radical anion  $\text{SO}_3^{\bullet -}$ , the concentration of which increased with time (Supporting Figure 2). Both  $\text{SO}_2^{\bullet -}$  and  $\text{H}_2\text{S}_2^{\bullet -}$  readily reduce  $\text{O}_2$  to form superoxide that can disproportionate to give  $\text{H}_2\text{O}_2$ .<sup>2,20</sup> The latter can oxidize ferrous Cyt C, enabling its redox

cycling.<sup>26,27</sup> Sulfite, peroxide, and heme proteins are known to produce  $\text{SO}_3^{\bullet-}$ , which is a potent oxidant that is proposed to play a role under certain pathological conditions.<sup>28–30</sup>  $\text{SO}_3^{\bullet-}$  could also contribute to Cyt C reoxidation to establish a pseudocatalytic cycle for  $\text{H}_2\text{S}$  removal.

### Cyt C Stimulates *in Vitro* Protein Persulfidation.

Protein thiols represent a potentially large pool of intracellular  $\text{HS}^{\bullet}/\text{S}^{\bullet-}$  scavengers (eq 7). To test the hypothesis that protein thiols are sinks for  $\text{HS}^{\bullet}/\text{S}^{\bullet-}$ , we first used time-resolved ESI-TOF-MS to monitor a reaction mixture containing Cyt C,  $\text{H}_2\text{S}$ , and cysteine. Formation of cysteine persulfide (as  $[\text{CysSSH} + \text{H}]^+$  and  $[2\text{CysSSH} + \text{H}]^+$  ions) and its decay products, CysSSCys (Figure 3A) and CysSSSCys (Supporting Figure 3A), was observed. While formation of CySSH plateaued within 1 min, formation of CysSSCys continued (Figure 3B and Supporting Figure 3B), supporting our previous report of the lability of CysSSH.<sup>31</sup>



Next, we tested Cyt C-dependent persulfidation of a model protein, human serum albumin (HSA). We have previously shown that addition of water-soluble heme iron and  $\text{H}_2\text{S}$  triggers protein persulfidation.<sup>32</sup> Incubation of HSA with sulfide in the presence of Cyt C also resulted in protein persulfidation (detected using the Cy3-CN-based tag switch method)<sup>33</sup> that was proportional to the concentration of Cyt C (Figure 3C). In contrast, when Cyt C was replaced with myoglobin, which oxidizes sulfide to polysulfides and thiosulfate via an inner sphere electron transfer mechanism, an increase in persulfidation was not observed (Supporting Figure 4). The residual persulfidation signals seen in the control lanes result from  $\text{H}_2\text{S}$ -induced reduction of the disulfide bond in HSA. We also demonstrated that the human mitochondrial proteins, ETHE-1 and adenosyltransferase (ATR), previously identified as persulfidation targets, were also persulfidated by Cyt C/ $\text{H}_2\text{S}$  (Figure 3D).

Interception of reactive sulfur species ( $\text{HS}^{\bullet}/\text{S}^{\bullet-}$ ) by cysteine residues on proteins should decrease the rate of Cyt C reduction by  $\text{H}_2\text{S}$  and  $\text{O}_2$  consumption. A substantial decrease in the rate of Cyt C reduction was in fact observed in the presence of equimolar HSA, which was attenuated by prior alkylation of HSA cysteines with iodoacetamide (Figure 3E). HSA also decreased the rate of  $\text{O}_2$  consumption, impacting both the burst and slow phases of the reaction (Figure 3F). Interestingly, the amplitude of the burst phase was increased in the presence of HSA. The initially formed  $\text{RSSH}^{\bullet-}$  protein radical anion is expected to be a strong reducing agent in analogy with  $\text{RSSR}^{\bullet-}$  [ $E^\circ'(\text{RSSR}/\text{RSSR}^{\bullet-}) = -1.4 \text{ V}$ ].<sup>34</sup> Because outer sphere electron transfer from the protein radical to Cyt C is likely to be precluded by steric hindrance,  $\text{O}_2$  would be the only available electron acceptor (eq 8), which could explain the higher amplitude observed for the burst phase (Figure 3F).



### Cyt C Silencing Decreases Intracellular Persulfidation.

To further investigate its role in protein persulfidation, Cyt C was silenced in HeLa cells. Under normoxic conditions, Cyt C silencing resulted in a small but statistically significant decrease in endogenous protein persulfidation as detected by the CN-Cy3-based tag switch method (Figure 4A). The mitochondrially targeted H<sub>2</sub>S donor AP39 caused a large increase in protein persulfidation as seen previously,<sup>33</sup> which was reduced by Cyt C siRNA treatment. The perinuclear localization of the persulfidation signal in AP39-treated cells confirms mitochondrial localization as reported for this donor.<sup>33,35,36</sup>

H<sub>2</sub>S oxidation is dependent on the presence of a functional ETC, and lower O<sub>2</sub> levels lead to H<sub>2</sub>S accumulation.<sup>37</sup> Using MeRho-Az, a bright fluorescence probe for H<sub>2</sub>S detection,<sup>35</sup> we observed a substantial increase in intracellular H<sub>2</sub>S in HeLa cells exposed to <5% O<sub>2</sub> (Figure 4B). A significant increase in protein persulfidation was observed in cells exposed to hypoxic conditions, which was diminished by silencing Cyt C (Figure 4C).

### Sulfide Stimulates O<sub>2</sub> Consumption in Complex III-Inhibited Cells.

To assess whether electrons from sulfide oxidation can bypass complex III and enter at the level of complex IV (Figure 5A), the O<sub>2</sub> consumption rate (OCR) was assessed with human cells in suspension. The OCR decreased to 2.5% (HepG2) and 5% (HT29) of the initial values in the presence of antimycin A, a complex III inhibitor (Figure 5B,C). Addition of sulfide (20 μM) increased the OCR by an average of 30% (HT29) and 95% (HepG2) above the antimycin-treated value. Higher concentrations of sulfide (100 μM) inhibited O<sub>2</sub> consumption as expected, presumably because of inhibition of complex IV. Addition of KCN, which poisons complex IV, blocked OCR, confirming that O<sub>2</sub> consumption induced by sulfide was linked to mitochondrial respiration.

Next, we assessed how inhibition of complex III and IV affects persulfidation in functional mitochondria that should produce H<sub>2</sub>S via the action of 3-mercaptopyruvate sulfurtransferase. Purified yeast mitochondria (*Saccharomyces cerevisiae*) treated with antimycin A showed an increase in intramitochondrial protein persulfidation, an effect that was inhibited by KCN (Figure 5D). This is in accordance with our hypothesis that even when H<sub>2</sub>S oxidation is inhibited by antimycin A, Cyt C-dependent consumption of H<sub>2</sub>S can still occur, leading to increased protein persulfidation. Inhibition of cytochrome *c* oxidase (by KCN), on the other hand, would prevent reoxidation of Cyt C and stop the cycle (Figure 5D).

Collectively, these results suggest that the canonical sulfide oxidation pathway can be bypassed to some extent by direct reduction of Cyt C. The reactive sulfur species formed under these conditions can react with protein thiols increasing persulfidation. We speculate that this situation could be particularly important in ischemia/reperfusion, protecting proteins from ROS-induced hyperoxidation during the reperfusion phase.

### Cyt C-Induced Persulfidation Controls Caspase 9 Activity.

In addition to its role in mitochondrial energy metabolism, Cyt C is an important regulator of apoptosis following its release into the cytosol.<sup>38,39</sup> In the presence of Cyt C, apoptotic

protease activating factors in the apoptosome activate procaspase 9, triggering a protease cascade.<sup>40</sup> Because of this functional association with Cyt C, we tested whether caspase 9, a cysteine protease, is persulfidated in the presence of H<sub>2</sub>S and Cyt C. Incubation with Cyt C and H<sub>2</sub>S stimulated persulfidation of recombinant murine procaspase 9 (Figure 6A). Next, we assessed caspase 9 activity in HeLa cell extracts using the fluorogenic caspase 9 substrate. Cyt C significantly stimulated caspase 9 activity, which was diminished in the presence of sulfide (Figure 6B).

Activity of caspase 9 in intact cells was also assessed by flow cytometry in Jurkat cells treated with staurosporine, an apoptosis inducer.<sup>41</sup> Staurosporine induced caspase 9 activity (Figure 6C), which was prevented by the slow-releasing H<sub>2</sub>S donor, 100  $\mu$ M GYY4137. In contrast, the faster-releasing H<sub>2</sub>S donor, ammonium tetrathiomolybdate, only partially inhibited the effect of staurosporine on caspase activation (Figure 6C).

Procaspase 3 is the downstream target of caspase 9, which cleaves it to the active caspase 3 form.<sup>42</sup> Induction of apoptosis by antimycin A treatment of HeLa cells for 16 h resulted in the expected increase in caspase 3 activity, which was partially inhibited by preincubating the cells for 2 h with GYY4137 (Figure 6D).

Finally, we checked whether persulfidation of procaspase 9 was affected in HeLa cells treated with staurosporine for 6 h. Cells were either pretreated with GYY4137 prior to staurosporine addition or treated for 2 h after induction of apoptosis by staurosporine (Supporting Figure 5A). GYY4137 treatment decreased total procaspase 9 levels (Figure 6E). Persulfidation of procaspase 9 was however significantly increased when the cells were treated with both staurosporine and the H<sub>2</sub>S donor (Figure 6E and Supporting Figure 5B).

Several caspases, including caspase 9, are inhibited by S-nitrosation of the active site cysteine.<sup>43,44</sup> Several mechanisms have been proposed to explain the antiapoptotic effects of sulfide.<sup>45,46</sup> We provide evidence that reactive sulfur species generated by Cyt C-mediated H<sub>2</sub>S oxidation can tag proteins with the cysteine persulfide modification. We posit that this reactivity might be enhanced under hypoxic conditions when H<sub>2</sub>S oxidation is inhibited or under apoptotic conditions when Cyt C is released into the cytoplasm and is disconnected from its mitochondrial electron donors, e.g., complex III. If H<sub>2</sub>S synthesis is upregulated under these conditions, persulfidation of protein targets in the proximity of Cyt C-like procaspase 9 will result. Inhibition of caspase 9 activity by persulfidation raises the possibility of designing peptidomimetic persulfide donors to inhibit its activity, similar to the reported S-nitrosothiol-containing peptide.<sup>47</sup>

In summary, we propose that the reaction between Cyt C and H<sub>2</sub>S results in the initial formation of a HS<sup>•</sup>/S<sup>•-</sup> radical. In a cellular milieu, HS<sup>•</sup>/S<sup>•-</sup> could suffer one of at least two fates: (i) be trapped by proteins, forming protein persulfides and superoxide, or (ii) be trapped by oxygen, forming HSO<sub>2</sub><sup>•</sup> (Figure 7). Dismutation of superoxide generated in scenario (i) would give H<sub>2</sub>O<sub>2</sub>, which together with H<sub>2</sub>S could lead to more persulfidation.<sup>48</sup> Formation of HSO<sub>2</sub><sup>•</sup> in scenario (ii) could further facilitate Cyt C reduction, resulting in sulfite and thiosulfate production. Cyt C reduction by H<sub>2</sub>S can fuel the ETC, bypassing complex III. Oxidation of Cyt C by complex IV would allow it to cycle between sulfide and

the ETC, potentially leading to the accumulation of reactive sulfur species. Cyt C-assisted protein persulfidation might represent a previously unrecognized source of reactive sulfur species that mediates the protective effects attributed to protein persulfidation.

## METHODS

### Reagents.

Antimycin A, equine heart ferric Cyt C, HSA, iodoacetamide, and Na<sub>2</sub>S nonahydrate (99.99%) were purchased from Sigma-Aldrich. Sodium disulfide (Na<sub>2</sub>S<sub>2</sub>) was from Dojindo Molecular Technologies, and monobromobimane FluoroPure grade was from Molecular Probes (Grand Island, NY). GYY4137, AP39, and MeRho-Az were synthesized in house as described previously.<sup>35,36,49</sup> 2-(Methylsulfonyl)-1,3-benzothiazole was from Santa Cruz Biotechnology, and CN-Cy3 was synthesized as reported previously.<sup>33</sup> Murine procaspase 9 was from Enzo Life Science. The siRNA for Cyt C was purchased from Santa Cruz Biotechnology. For the anaerobic experiments, buffers were purged with argon. To maintain high purity, Na<sub>2</sub>S solutions were made in an argon box by dissolving solid Na<sub>2</sub>S·9H<sub>2</sub>O into argon-purged water, as recommended.<sup>2,19</sup>

### Cell Culture.

Human colon cancer (HT29), hepatocellular carcinoma (HepG2), cervical cancer (HeLa), and immortalized human T-lymphocyte (Jurkat) cell lines were purchased from ATCC. Cells were cultured in 10 cm plates in EMEM (HepG2) or RPMI 1640 (HT29) supplemented with 10% FBS (Gibco) and a 1% penicillin (10000 units mL<sup>-1</sup>)/streptomycin (10000 μg mL<sup>-1</sup>) mixture (Gibco). Jurkat and HeLa cells were cultured in 75 cm flasks in complete RPMI medium and DMEM (Sigma-Aldrich), respectively, supplemented with 10% FBS and a 1% penicillin (10000 units mL<sup>-1</sup>)/streptomycin (10000 μg mL<sup>-1</sup>) mixture (Sigma-Aldrich).

A detailed description of the methods is given in the Supporting Information.

## Supplementary Material

Refer to Web version on PubMed Central for supplementary material.

## ACKNOWLEDGMENTS

This work was supported by the French State in the frame of the “Investments for the future” Programme IdEx Bordeaux, reference ANR-10-IDEX-03-02, and by an ATIP-AVENIR grant (to M.R.F.), the National Institutes of Health (GM112455 to R.B. and R01GM113030 to M.D.P.), the Medical Research Council, UK (MR/M022706/1 to M.W.), the National Science Foundation (DGE-1309047 to A.K.S.), and the Brian Ridge Scholarship (R.T.). The authors are grateful to M.-F. Giraud for the help with purification of mitochondria.

## REFERENCES

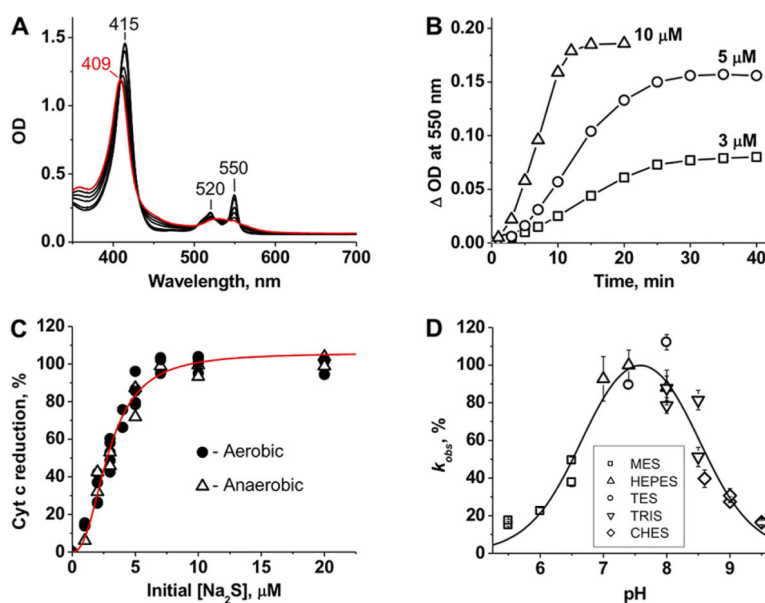
- (1). Keilin D (1929) Cytochrome and Respiratory Enzymes. Proc. R. Soc. London, Ser. B 104, 206–252.
- (2). Filipovic MR, Zivanovic J, Alvarez B, and Banerjee R (2018) Chemical Biology of H<sub>2</sub>S Signaling through Persulfidation. Chem. Rev 118, 1253–1337. [PubMed: 29112440]
- (3). Kimura H (2010) Hydrogen Sulfide: From Brain to Gut. Antioxid. Redox Signaling 12, 1111–1123.



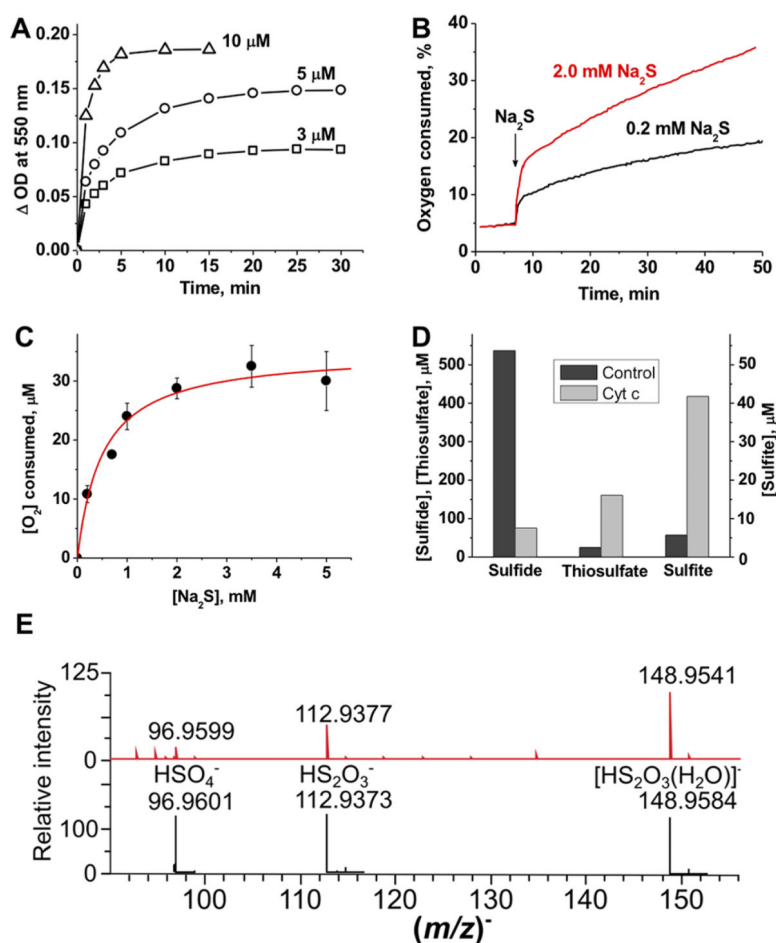
- (4). Kabil O, and Banerjee R (2010) Redox Biochemistry of Hydrogen Sulfide. *J. Biol. Chem* 285, 21903–21907. [PubMed: 20448039]
- (5). Kabil O, Motl N, and Banerjee R (2014) H<sub>2</sub>S and its role in redox signaling. *Biochim. Biophys. Acta, Proteins Proteomics* 1844, 1355–1366.
- (6). Singh S, Padovani D, Leslie RA, Chiku T, and Banerjee R (2009) Relative Contributions of Cystathionine  $\beta$ -Synthase and  $\gamma$ -Cystathionase to H<sub>2</sub>S Biogenesis via Alternative Transsulfuration Reactions. *J. Biol. Chem* 284, 22457–22466. [PubMed: 19531479]
- (7). Chiku T, Padovani D, Zhu W, Singh S, Vitvitsky V, and Banerjee R (2009) H<sub>2</sub>S Biogenesis by Human Cystathionine gamma-Lyase Leads to the Novel Sulfur Metabolites Lanthionine and Homolanthionine and Is Responsive to the Grade of Hyper-homocysteinemia. *J. Biol. Chem* 284, 11601–11612. [PubMed: 19261609]
- (8). Shibuya N, Tanaka M, Yoshida M, Ogasawara Y, Togawa T, Ishii K, and Kimura H (2009) 3-Mercaptopyruvate Sulfur-transferase Produces Hydrogen Sulfide and Bound Sulfane Sulfur in the Brain. *Antioxid. Redox Signaling* 11, 703–714.
- (9). Yadav PK, Yamada K, Chiku T, Koutmos M, and Banerjee R (2013) Structure and Kinetic Analysis of H<sub>2</sub>S Production by Human Mercaptopyruvate Sulfurtransferase. *J. Biol. Chem* 288, 20002–20013. [PubMed: 23698001]
- (10). Kabil O, and Banerjee R (2012) Characterization of Patient Mutations in Human Persulfide Dioxygenase (ETHE1) Involved in H<sub>2</sub>S Catabolism. *J. Biol. Chem* 287, 44561–44567. [PubMed: 23144459]
- (11). Kabil O, Vitvitsky V, and Banerjee R (2014) Sulfur as a Signaling Nutrient Through Hydrogen Sulfide. *Annu. Rev. Nutr* 34, 171–205. [PubMed: 25033061]
- (12). Hildebrandt TM, and Grieshaber MK (2008) Three enzymatic activities catalyze the oxidation of sulfide to thiosulfate in mammalian and invertebrate mitochondria. *FEBS J.* 275, 3352–3361. [PubMed: 18494801]
- (13). Vitvitsky V, Yadav PK, Kurthen A, and Banerjee R (2015) Sulfide Oxidation by a Noncanonical Pathway in Red Blood Cells Generates Thiosulfate and Polysulfides. *J. Biol. Chem* 290, 8310–8320. [PubMed: 25688092]
- (14). Vitvitsky V, Yadav PK, An S, Seravalli J, Cho U-S, and Banerjee R (2017) Structural and Mechanistic Insights into Hemoglobin-catalyzed Hydrogen Sulfide Oxidation and the Fate of Polysulfide Products. *J. Biol. Chem* 292, 5584–5592. [PubMed: 28213526]
- (15). Bostelaar T, Vitvitsky V, Kumutima J, Lewis BE, Yadav PK, Brunold TC, Filipovic M, Lehnert N, Stemmler TL, and Banerjee R (2016) Hydrogen Sulfide Oxidation by Myoglobin. *J. Am. Chem. Soc* 138, 8476–8488. [PubMed: 27310035]
- (16). Ruetz M, Kumutima J, Lewis BE, Filipovic MR, Lehnert N, Stemmler TL, and Banerjee R (2017) A distal ligand mutes the interaction of hydrogen sulfide with human neuroglobin. *J. Biol. Chem* 292, 6512–6528. [PubMed: 28246171]
- (17). Riedl SJ, and Salvesen GS (2007) The apoptosome: Signalling platform of cell death. *Nat. Rev. Mol. Cell Biol* 8, 405–413. [PubMed: 17377525]
- (18). Nicholls P, and Kim JK (1981) Oxidation of sulphide by cytochrome aa<sub>3</sub>. *Biochim. Biophys. Acta, Bioenerg* 637, 312–320.
- (19). Wedmann R, Bertlein S, Macinkovic I, Böltz S, Miljkovic JL, Muñoz LE, Herrmann M, and Filipovic MR (2014) Working with “H<sub>2</sub>S”: Facts and apparent artifacts. *Nitric Oxide* 41, 85–96. [PubMed: 24932545]
- (20). Koppenol WH, and Bounds PL (2017) Signaling by sulfur-containing molecules. Quantitative aspects. *Arch. Biochem. Biophys* 617, 3–8. [PubMed: 27670814]
- (21). Battistuzzi G, Borsari M, Cowan JA, Ranieri A, and Sola M (2002) Control of cytochrome c redox potential: Axial ligation and protein environment effects. *J. Am. Chem. Soc* 124, 5315–5324. [PubMed: 11996572]
- (22). Collman JP, Ghosh S, Dey A, and Decreau RA (2009) Using a functional enzyme model to understand the chemistry behind hydrogen sulfide induced hibernation. *Proc. Natl. Acad. Sci. U. S. A* 106, 22090–22095. [PubMed: 20007376]

- (23). Doeller JE, Grieshaber MK, and Kraus DW (2001) Chemolithoheterotrophy in a metazoan tissue: thiosulfate production matches ATP demand in ciliated mussel gills. *J. Exp. Biol* 204, 3755–3764. [PubMed: 11719539]
- (24). Hu L, Lu M, Wu Z, Wong PT-H, and Bian J (2009) Hydrogen sulfide inhibits rotenone-induced apoptosis via preservation of mitochondrial function. *Mol. Pharmacol* 75, 27–34. [PubMed: 18832435]
- (25). Battistuzzi G, Borsari M, Dallari D, Lancellotti I, and Sola M (1996) Anion binding to mitochondrial cytochromes c studied through electrochemistry Effects of the neutralization of surface charges on the redox potential. *Eur. J. Biochem* 241, 208–214. [PubMed: 8898908]
- (26). Radi R, Thomson L, Rubbo H, and Prodanov E (1991) Cytochrome c-catalyzed oxidation of organic molecules by hydrogen peroxide. *Arch. Biochem. Biophys* 288, 112–117. [PubMed: 1654817]
- (27). Alvarez-Paggi D, Hannibal L, Castro MA, Oviedo-Rouco S, Demicheli V, Tórtora V, Tomasina F, Radi R, and Murgida DH (2017) Multifunctional Cytochrome c: Learning New Tricks from an Old Dog. *Chem. Rev* 117, 13382–13460. [PubMed: 29027792]
- (28). Mottley C, Mason RP, Chignell CF, Sivarajah K, and Eling TE (1982) The formation of sulfur trioxide radical anion during the prostaglandin hydroperoxidase-catalyzed oxidation of bisulfite (hydrated sulfur dioxide). *J. Biol. Chem* 257, 5050–5055. [PubMed: 6279657]
- (29). Neta P, and Huie RE (1985) Free-radical chemistry of sulfite. *Environ. Health Perspect* 64, 209–217. [PubMed: 3830699]
- (30). Mottley C, Trice TB, and Mason RP (1982) Direct detection of the sulfur trioxide radical anion during the horseradish peroxidase-hydrogen peroxide oxidation of sulfite (aqueous sulfur dioxide). *Mol. Pharmacol* 22, 732–737. [PubMed: 6296662]
- (31). Yadav PK, Martinov M, Vitvitsky V, Seravalli J, Wedmann R, Filipovic MR, and Banerjee R (2016) Biosynthesis and Reactivity of Cysteine Persulfides in Signaling. *J. Am. Chem. Soc* 138, 289–299. [PubMed: 26667407]
- (32). Zhang D, MacInkovic I, Devarie-Baez NO, Pan J, Park C-M, Carroll KS, Filipovic MR, and Xian M (2014) Detection of protein S-sulfhydration by a tag-switch technique. *Angew. Chem., Int. Ed* 53, 575–581.
- (33). Wedmann R, Onderka C, Wei S, Szijártó IA, Miljkovic JL, Mitrovic A, Lange M, Savitsky S, Yadav PK, Torregrossa R, Harrer EG, Harrer T, Ishii I, Gollasch M, Wood ME, Galardon E, Xian M, Whiteman M, Banerjee R, and Filipovic MR (2016) Improved tag-switch method reveals that thioredoxin acts as depersulfidase and controls the intracellular levels of protein persulfidation. *Chem. Sci* 7, 3414–3426. [PubMed: 27170841]
- (34). Buettner GR (1993) The Pecking Order of Free Radicals and Antioxidants: Lipid Peroxidation,  $\alpha$ -Tocopherol, and Ascorbate. *Arch. Biochem. Biophys* 300, 535–543. [PubMed: 8434935]
- (35). Hammers MD, Taormina MJ, Cerda MM, Montoya LA, Seidenkranz DT, Parthasarathy R, and Pluth MD (2015) A Bright Fluorescent Probe for H<sub>2</sub>S Enables Analyte-Responsive, 3D Imaging in Live Zebrafish Using Light Sheet Fluorescence Microscopy. *J. Am. Chem. Soc* 137, 10216–10223. [PubMed: 26061541]
- (36). Le Trionnaire S, Perry A, Szczesny B, Szabo C, Winyard PG, Whatmore JL, Wood ME, and Whiteman M (2014) The synthesis and functional evaluation of a mitochondria-targeted hydrogen sulfide donor, (10-oxo-10-(4-(3-thioxo-3H-1,2-dithiol-5-yl)phenoxy)decyl)triphenylphosphonium bromide (AP39). *MedChemComm* 5, 728–736.
- (37). Arndt S, Baeza-Garza CD, Logan A, Rosa T, Wedmann R, Prime TA, Martin JL, Saeb-Parsy K, Krieg T, Filipovic MR, Hartley RC, and Murphy MP (2017) Assessment of H<sub>2</sub>S in vivo using the newly developed mitochondria-targeted mass spectrometry probe MitoA. *J. Biol. Chem* 292, 7761–7773. [PubMed: 28320864]
- (38). Garrido C, Galluzzi L, Brunet M, Puig PE, Didelot C, and Kroemer G (2006) Mechanisms of cytochrome c release from mitochondria. *Cell Death Differ.* 13, 1423–1433. [PubMed: 16676004]
- (39). Cai J, Yang J, and Jones DP (1998) Mitochondrial control of apoptosis: the role of cytochrome c. *Biochim. Biophys. Acta, Bioenerg* 1366, 139–149.

- (40). Li P, Nijhawan D, Budihardjo I, Srinivasula SM, Ahmad M, Alnemri ES, and Wang X (1997) Cytochrome c and dATP-dependent formation of Apaf-1/caspase-9 complex initiates an apoptotic protease cascade. *Cell* 91, 479–489. [PubMed: 9390557]
- (41). Luetjens CM, Kögel D, Reimertz C, Düßmann H, Renz A, Schulze-Osthoff K, Nieminen A-L, Poppe M, and Prehn JHM (2001) Multiple kinetics of mitochondrial cytochrome c release in drug-induced apoptosis. *Mol. Pharmacol* 60, 1008–1019. [PubMed: 11641429]
- (42). Zou H, Yang R, Hao J, Wang J, Sun C, Fesik SW, Wu JC, Tomaselli KJ, and Armstrong RC (2003) Regulation of the Apaf-1/Caspase 9 apoptosome by Caspase-3 and XIAP. *J. Biol. Chem* 278, 8091–8098. [PubMed: 12506111]
- (43). Kim J-E, and Tannenbaum SR (2004) S-Nitrosation regulates the activation of endogenous procaspase-9 in HT-29 human colon carcinoma cells. *J. Biol. Chem* 279, 9758–9764. [PubMed: 14701803]
- (44). Mannick JB, Schonhoff C, Papeta N, Ghafourifar P, Szibor M, Fang K, and Gaston B (2001) S-nitrosylation of mitochondrial caspases. *J. Cell Biol* 154, 1111–1116. [PubMed: 11551979]
- (45). Sivarajah A, Collino M, Yasin M, Benetti E, Gallicchio M, Mazzon E, Cuzzocrea S, Fantozzi R, and Thiemermann C (2009) Anti-apoptotic and anti-inflammatory effects of hydrogen sulfide in a rat model of regional myocardial I/R. *Shock* 31, 267–274. [PubMed: 18636044]
- (46). Sen N, Paul BD, Gadalla MM, Mustafa AK, Sen T, Xu R, Kim S, and Snyder SH (2012) Hydrogen sulfide-linked sulfhydration of NF- $\kappa$ B mediates its antiapoptotic actions. *Mol. Cell* 45, 13–24. [PubMed: 22244329]
- (47). Mitchell DA, Morton SU, and Marletta MA (2006) Design and characterization of an active site selective caspase-3 transnitrosating agent. *ACS Chem. Biol* 1, 659–665. [PubMed: 17168570]
- (48). Cuevasanta E, Lange M, Bonanata J, Coitiño EL, Ferrer-Sueta G, Filipovic MR, and Alvarez B (2015) Reaction of hydrogen sulfide with disulfide and Sulfenic acid to form the strongly Nucleophilic Persulfide. *J. Biol. Chem* 290, 26866–26880. [PubMed: 26269587]
- (49). Alexander BE, Coles SJ, Fox BC, Khan TF, Maliszewski J, Perry A, Pitak MB, Whiteman M, and Wood ME (2015) Investigating the generation of hydrogen sulfide from the phosphonamidodithioate slow-release donor GYY4137. *MedChemComm* 6, 1649–1655.



**Figure 1.** Reduction of Cyt C by sulfide. (A) The initial spectrum of ferric Cyt C ( $10 \mu\text{M}$ ) in  $100 \text{ mM}$  HEPES buffer [ $\text{pH } 7.4$  (red)] shifts in the presence of  $10 \mu\text{M}$   $\text{Na}_2\text{S}$  (at 3, 5, 7, 10, 15, and 20 min, black lines) under aerobic conditions at  $25 \text{ }^\circ\text{C}$ . (B) Kinetics of aerobic Cyt C reduction ( $10 \mu\text{M}$ ) at 3, 5, and  $10 \mu\text{M}$   $\text{Na}_2\text{S}$  in  $100 \text{ mM}$  HEPES buffer ( $\text{pH } 7.4$ ) at  $25 \text{ }^\circ\text{C}$ . (C) Percent Cyt C [ $10 \mu\text{M}$  in  $100 \text{ mM}$  HEPES buffer ( $\text{pH } 7.4$ )] reduction as a function of sulfide concentration. The increase in absorbance at  $550 \text{ nm}$  was monitored after incubation with sulfide at  $25 \text{ }^\circ\text{C}$  for 1 h under aerobic or anaerobic conditions. The red line is a sigmoidal fit to the experimental data with an  $S_{0.5}$  of  $2.9 \pm 0.1 \mu\text{M}$  and an  $n$  of  $2.4 \pm 0.2$ . (D) pH dependence of Cyt C reduction by sulfide. The rate of Cyt C ( $2.5 \mu\text{M}$ ) reduction by sulfide ( $500 \mu\text{M}$ ) was determined by anaerobic stopped-flow spectroscopy as described in Methods. The data are the mean  $\pm$  the standard deviation (SD) of four independent experiments as described in Methods. From the fit, estimates for  $\text{p}K_{a1}$  and  $\text{p}K_{a2}$  of  $6.7 \pm 0.1$  and  $8.5 \pm 0.1$ , respectively, were obtained.

**Figure 2.**

Cyt C reduction kinetics and product analysis. (A) Kinetics of aerobic Cyt C reduction (10  $\mu\text{M}$ ) in the presence of 3, 5, and 10  $\mu\text{M}$   $\text{Na}_2\text{S}_2$  in 100 mM HEPES buffer (pH 7.4) at 25  $^\circ\text{C}$ . Complete reduction with equimolar  $\text{Na}_2\text{S}_2$  was seen within 5–10 min. (B) Kinetics of  $\text{O}_2$  consumption in the presence of Cyt C and sulfide. Addition of sulfide to Cyt C [50  $\mu\text{M}$  in 100 mM HEPES buffer (pH 7.4)] at 25  $^\circ\text{C}$  results in rapid initial consumption of  $\text{O}_2$  followed by a slower phase. (C) Dependence of the concentration of  $\text{O}_2$  consumed in the burst phase on sulfide concentration. A hyperbolic fit to the data (mean  $\pm$  SD of three to five independent experiments) gives a  $K_{\text{act}}$  of  $0.5 \pm 0.1$  mM and a maximal  $\text{O}_2$  consumed of  $35 \pm 2$   $\mu\text{M}$  (red line), yielding a  $\text{O}_2$  consumed:Cyt C stoichiometry of 0.7:1.0. (D) Consumption of sulfide and accumulation of thiosulfate and sulfite 2 h after addition of 800  $\mu\text{M}$   $\text{Na}_2\text{S}$  to 100 mM HEPES buffer (pH 7.4) without (black bars) or with (gray bars) 100  $\mu\text{M}$  Cyt C at 25  $^\circ\text{C}$  under aerobic conditions. The initial levels of sulfide, thiosulfate, and sulfite were 756, 25, and 3.5  $\mu\text{M}$ , respectively. (E) MS detection of sulfur products formed in the reaction of 10  $\mu\text{M}$  Cyt C with 100  $\mu\text{M}$   $\text{H}_2\text{S}$  in ammonium carbonate buffer (pH 7.7) under aerobic conditions. The reaction was monitored for 15 min at room temperature. The observed spectrum is at the top, and the simulated spectra with an isotopic distribution are below.

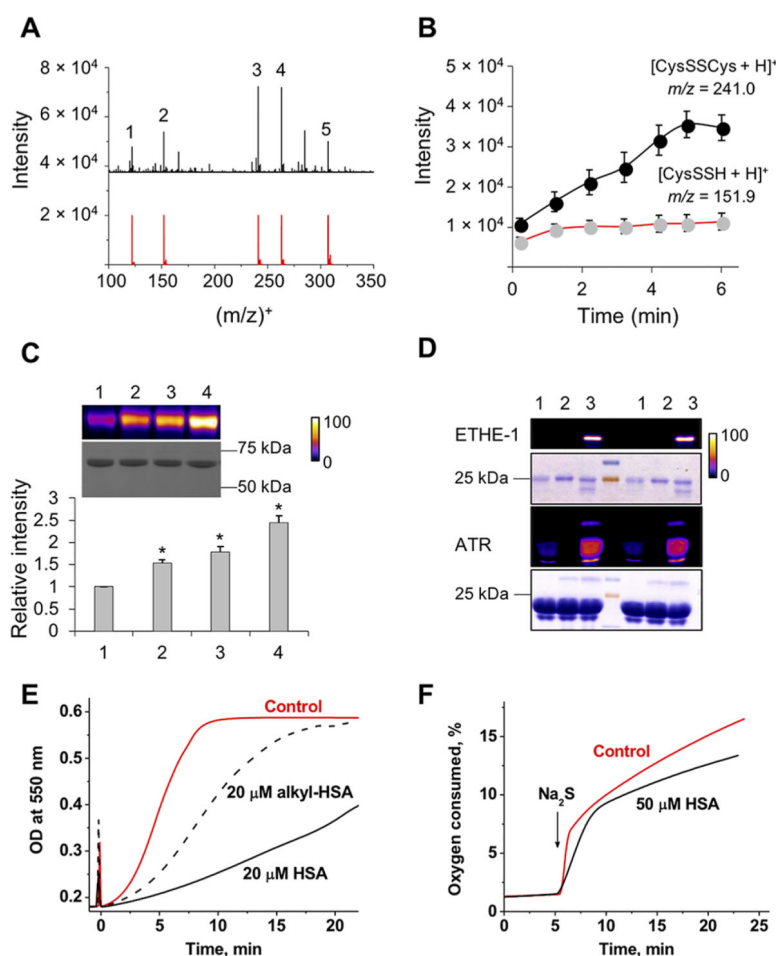


**Figure 3.** Cyt C stimulates H<sub>2</sub>S-dependent persulfidation. (A) Mass spectrum of the reaction mixture ( $t = 6$  min) containing 20  $\mu\text{M}$  Cyt C, 100  $\mu\text{M}$  H<sub>2</sub>S, and 200  $\mu\text{M}$  cysteine in ammonium carbonate buffer (pH 7.7) at 21 °C and simulated isotopic distributions for some of the identified species: 1, [CysSH + H]<sup>+</sup>; 2, [CysSSH + H]<sup>+</sup>; 3, [CysSSCys + H]<sup>+</sup>; 4, [CysSSCys + Na]<sup>+</sup>; 5, [2CysSSH + H]<sup>+</sup>. (B) Kinetics of [CysSSH + H]<sup>+</sup> ( $m/z$  151.9) and [CysSSCys + H]<sup>+</sup> ( $m/z$  241.0) formation. Data represent means  $\pm$  SD of three independent experiments. (C) Persulfidation of HSA (10  $\mu\text{M}$ ) in phosphate-buffered saline (pH 7.4), incubated for 30 min at room temperature with 500  $\mu\text{M}$  Na<sub>2</sub>S (lane 1) and 2  $\mu\text{M}$  (lane 2), 20  $\mu\text{M}$  (lane 3), and 200  $\mu\text{M}$  (lane 4) Cyt C. Data represent means  $\pm$  SD ( $n = 3$ ; \* $p < 0.001$ ). (D) Persulfidation of purified (1  $\mu\text{M}$ ) ETHE-1 and (10  $\mu\text{M}$ ) ATR treated with either 100  $\mu\text{M}$  H<sub>2</sub>S (lane 1), 10  $\mu\text{M}$  Cyt C (lane 2), or combination of both (lane 3). The results of two separate experiments are shown. Persulfidation (C and D) was detected by the CN-Cy3-based tag switch method (top panels), while equal loading was detected by Coomassie blue staining (bottom panels). The gel was artificially colorized using ImageJ to enhanced visualization of changes, and the fluorescence intensity scale is provided on the right. The persulfidation procedure is described in Supporting Materials and Methods. (E) Aerobic kinetics of Cyt C [20  $\mu\text{M}$  in 100 mM HEPES buffer (pH 7.4) at 25 °C] reduction (monitored at 550 nm) by Na<sub>2</sub>S (20  $\mu\text{M}$ ) with or without untreated or alkylated HSA (20  $\mu\text{M}$ ). Sulfide was added at time zero.

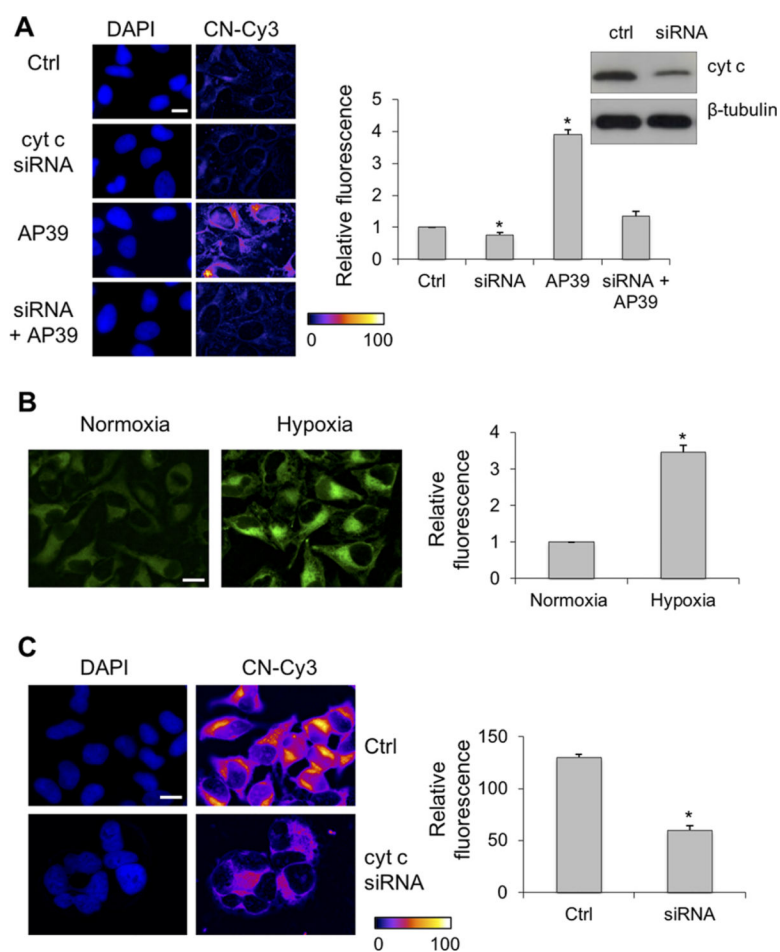
(F) Kinetics of O<sub>2</sub> consumption after addition of 0.2 mM Na<sub>2</sub>S to ferric Cyt C [50 μM in 100 mM HEPES buffer (pH 7.4)] with or without 50 μM HSA at 25 °C.

Author Manuscript

Author Manuscript

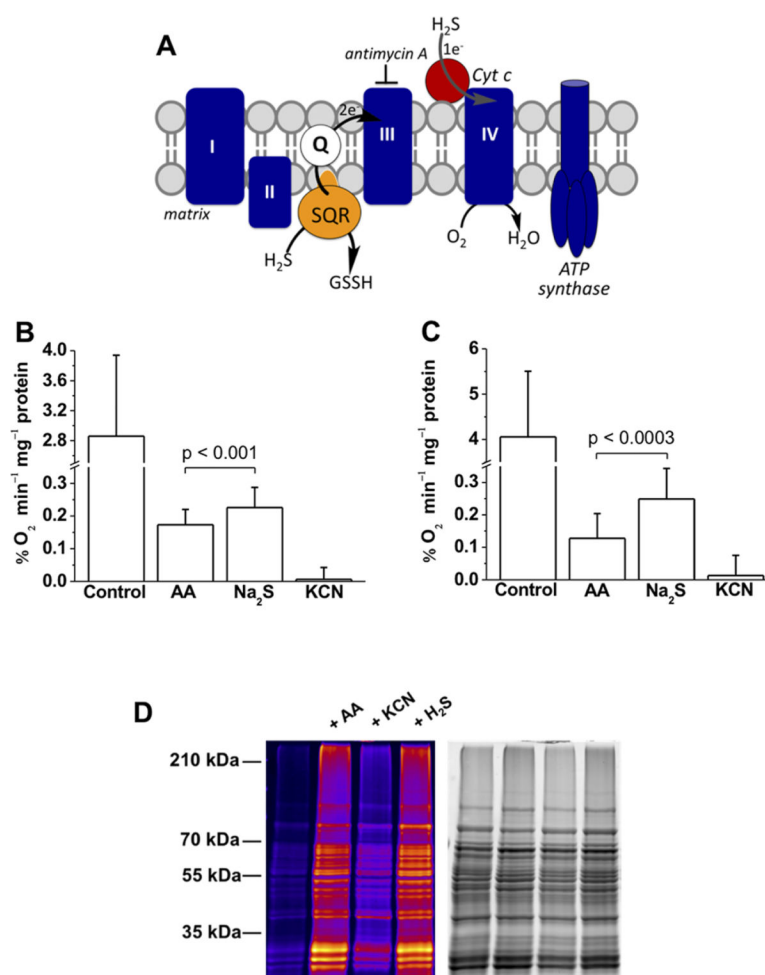
Author Manuscript

Author Manuscript

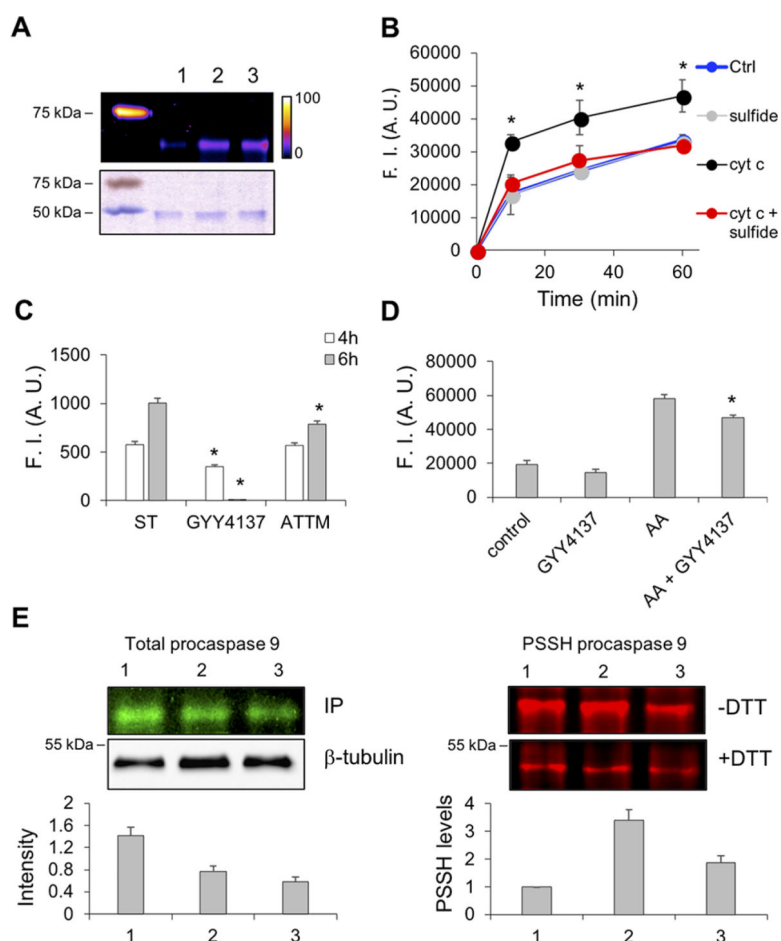


**Figure 4.** Cyt C silencing decreases protein persulfidation. (A) Under normoxic conditions, silencing of Cyt C in HeLa cells (confirmed by Western blot analysis) led to a small but measurable decrease in basal persulfidation levels, which was increased by the mitochondrially targeted H<sub>2</sub>S donor, AP39 (200 nM). The scale bar is 5  $\mu$ m. (B) Exposure of HeLa cells to hypoxia for 1 h results in increased endogenous H<sub>2</sub>S levels as detected by MerRho-Az. The scale bar is 10  $\mu$ m. (C) Under hypoxic conditions, the levels of protein persulfidation are high but significantly reduced by Cyt C silencing. The scale bar is 10  $\mu$ m. Representative microscopy images are given on the left, and quantitative image analysis is given on the right. The results represent the average fluorescence intensity (F. I.) detected from 40 cells  $\pm$  the standard error of the mean of five independent images (\* $p$  < 0.001).





**Figure 5.** Sulfide stimulates O<sub>2</sub> consumption by mammalian cells and controls persulfidation of mitochondrial proteins. (A) Cartoon showing electrons from H<sub>2</sub>S oxidation enter the ETC at the level of complex III via the reduced quinone pool. Entry into complex IV via Cyt C can be monitored in the presence of antimycin A, a complex III inhibitor. (B and C) O<sub>2</sub> consumption rates of HT29 and HepG2 cells, respectively, before (control) and after treatment with 2 μg mL<sup>-1</sup> antimycin A (AA) followed by 20 μM Na<sub>2</sub>S. Finally, antimycin A-treated cells were exposed to 5 mM KCN. The data are means ± SD of 12 (B) or 6 (C) independent experiments; the *p* value shows the statistical significance for the difference between antimycin A with and without sulfide-treated cells. (D) Protein persulfidation in purified mitochondria is affected by the ETC. Functional mitochondria were isolated from *S. cerevisiae* and preincubated with 2.5 μg mL<sup>-1</sup> antimycin A or 10 mM KCN for 10 min at 37 °C or treated with 1 μM H<sub>2</sub>S for 20 min at 37 °C. Persulfidation was monitored by the improved tag switch method. The first lane represents the basal persulfidation level in untreated functional mitochondria. The total protein load is shown in the gel on the right.

**Figure 6.**

Cyt C mediates procaspase 9 persulfidation and activity. (A) Murine recombinant procaspase 9 ( $1 \mu\text{M}$ ) was incubated with  $5 \mu\text{M}$   $\text{H}_2\text{S}$  for 30 min at  $37^\circ\text{C}$  in the absence (lane 1) or presence of  $0.5$  (lane 2) and  $2 \mu\text{M}$  (lane 3) Cyt C. Persulfidation was detected by the CN-Cy3-based tag switch method (top panel), while equal loading was confirmed by Coomassie blue staining (bottom panel). (B)  $\text{H}_2\text{S}$  inhibits Cyt C-induced caspase 9 activation in cell lysates. Cyt C ( $500 \text{ nM}$ ) was added to freshly prepared HeLa cell lysates, and caspase 9 activity was monitored using a fluorescence caspase 9 kit. Simultaneous addition of Cyt C and  $\text{H}_2\text{S}$  ( $10 \mu\text{M}$ ) inhibited the Cyt C-induced increase in fluorescence. (C) Cyt C-induced caspase 9 activation in Jurkat cells is inhibited by  $\text{H}_2\text{S}$  donors. Apoptosis was induced by staurosporine (ST,  $2.5 \mu\text{M}$ ), and caspase 9 activity was monitored by flow cytometry using the caspase 9 FITC staining kit 4 and 6 h after induction. Treatment of cells with GYY4137 ( $100 \mu\text{M}$ ) or ammonium tetrathiomolybdate (ATTM,  $200 \mu\text{M}$ ) reduced fluorescence. (D) Inhibition of caspase 3 activation in cells treated with antimycin A and the slow-releasing  $\text{H}_2\text{S}$  donor, GYY4137 ( $100 \mu\text{M}$ ). HeLa cells were incubated with antimycin A ( $300 \mu\text{M}$ ) overnight to induce the release of Cyt C from mitochondria. GYY4137, when used, was added 2 h prior to antimycin A. Caspase 3 activity was monitored in cell lysates as described for panel B. (E) Persulfidation of procaspase 9 in HeLa cells treated with  $2.5 \mu\text{M}$  ST (1) that were either pretreated for 2 h (2) or treated for the last 2 h (3) with GYY4137 ( $100 \mu\text{M}$ ):

(left) total procaspase 9 levels and (right) persulfidation (PSSH) levels of procaspase 9. PSSH levels were quantified by measuring the difference in fluorescence between DTT-treated and untreated samples and normalizing this to the total procaspase 9 levels. The strategy used for sample processing to detect total versus persulfidated procaspase 9 is explained in the Supporting Information and Supporting Figure 5.

Author Manuscript

Author Manuscript

Author Manuscript

Author Manuscript

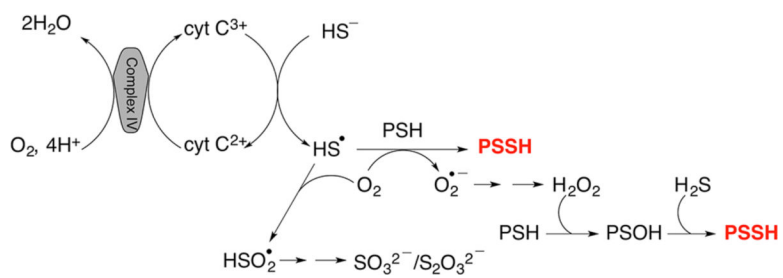


**Figure 7.**  
Protein persulfidation catalyzed by the Cyt C/H<sub>2</sub>S couple.